

COHERENT UNDULATOR RADIATION FROM A KICKED ELECTRON BEAM

J. P. MacArthur*, A. A. Lutman, J. Krzywinski, Z. Huang,
SLAC National Accelerator Laboratory, Menlo Park, USA

Abstract

The properties of off-axis radiation from an electron beam that has been kicked off axis are relevant to recent Delta undulator experiments at LCLS. We calculate the coherent emission from a microbunched beam in the far-field, and compare with simulation. We also present a mechanism for microbunches to tilt toward a new direction of propagation.

INTRODUCTION

During the commissioning of the Delta undulator at LCLS, a highly circularly polarized beam was produced by kicking the electron beam prior to the Delta undulator [1]. This situation is depicted in Figure 1. With the right detune in the Delta undulator parameter K , a large angular separation between linear light produced prior to the Delta and circular light produced in the Delta was observed. This result is non-intuitive because, as seen in Figure 1, the microbunches don't realign themselves in the direction of propagation.

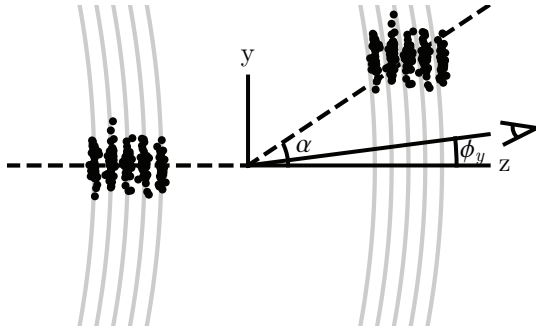


Figure 1: Microbunched electrons traveling left to right (black) are kicked by an angle $\alpha \ll 1$ in the y direction. The microbunches drift relative to the extant electric field (gray). An observer examines the far-field power at an angle ϕ_y .

Here the coherent radiation from a kicked beam is analyzed from a classical synchrotron radiation perspective. The motion of an electron in a diffracting electric field is also investigated.

COHERENT EMISSION FROM ANGLED MICROBUNCHES

The electric field in the paraxial approximation from a single electron traveling on axis and with no transverse velocity in an undulator of length L_u is [2]

$$\mathcal{E}_{v,j}^0(\phi, z = L_u) \propto e^{i\omega t_j} \int_0^{L_u} e^{ikz'\phi^2/2} e^{i(\nu-1)k_u z'} dz', \quad (1)$$

* jmacart@slac.stanford.edu

where $\mathcal{E}_{v,j}^0(\phi, z)$ is the field at an angle ϕ and wavenumber $k = \omega/c = \nu k_1$, t_j is the electron arrival time at $z = 0$, and k_1 is the wavenumber resonant to an undulator of period $\lambda_u = 2\pi/k_u$. The frequency of interest is detuned by an amount $\Delta\nu = \nu - 1 = (k - k_1)/k_1$ from the undulator resonant frequency.

The electric field from an electron with position \mathbf{x}_j , transverse velocity $d\mathbf{x}_j/dz = \mathbf{x}'_j$, and energy deviation from resonance $\eta_j = (\gamma - \gamma_r)/\gamma_r$ is [2]

$$\mathcal{E}_{v,j}(\phi, L_u) = e^{-ik\phi \cdot \mathbf{x}_j} \mathcal{E}_{\nu-2\eta_j,j}^0(\phi - \mathbf{x}'_j, L_u). \quad (2)$$

In order to calculate the power from the kicked beam shown in Figure 1, we sum and square the contributions from all N_e electrons,

$$P(\phi, L_u) = \sum_j^{N_e} |\mathcal{E}_{v,j}|^2 + \sum_j^{N_e} \sum_{k \neq j}^{N_e} \mathcal{E}_{v,j} \mathcal{E}_{v,k}^*. \quad (3)$$

The first sum is inconsequential for a bunched beam, while the double sum is typically converted into a double integral over the electron probability distribution, $f(\mathbf{x}_j, \mathbf{x}'_j, \eta_j, t_j)$.

For simplicity we assume that all variables are independent and therefore f is separable. The expression for the power takes a simple form when the beam has no spread in energy ($\eta_j = 0$), and no spread in angle ($\mathbf{x}'_j = 0$). These assumptions eliminate the emittance effects discussed in Ref [3], but other effects become more apparent. To match Figure 1, we set $\mathbf{x}'_j = (0, \alpha)$. The explicit form of the longitudinal distribution $f(t_j)$ is not important for this calculation, so we set

$$\int e^{i\omega t} f(t) dt = b. \quad (4)$$

After integrating over \mathbf{x} and t , the power is seen to be

$$P(\phi_x, \phi_y) \propto |b|^2 |\tilde{f}(\phi_x, \phi_y)|^2 \times \text{sinc}^2 \left[\pi N_u \left(\Delta\nu + \gamma_z^2 \phi_x^2 + \gamma_z^2 (\phi_y - \alpha)^2 \right) \right], \quad (5)$$

where

$$\tilde{f}(\phi_x, \phi_y) = \int d\mathbf{x} f(x, y) e^{ik\phi \cdot \mathbf{x}} \quad (6)$$

is the spatial transform of the transverse distribution, $N_u = L_u/\lambda_u$ is the number of oscillations in the wiggler, and $\gamma_z^2 = \gamma^2/(1 + K^2)$. Expressions similar to Equation 5 are derived elsewhere [3–5]. If \mathbf{x} is normally distributed around zero with rms spread σ ,

$$P(\phi_x, \phi_y) \propto |b|^2 e^{-k^2 \sigma^2 (\phi_x^2 + \phi_y^2)} \times \text{sinc}^2 \left[\pi N_u \left(\Delta\nu + \gamma_z^2 \phi_x^2 + \gamma_z^2 (\phi_y - \alpha)^2 \right) \right], \quad (7)$$

Examining Equation 7, the far-field intensity may be maximized by setting the argument of the sinc function equal to zero with $\phi = 0$. The detune Δv^* required to correct for a tilt α is

$$\Delta v^* = -\gamma_z^2 \alpha^2. \quad (8)$$

This prediction is compared to Genesis simulation results in a subsequent section.

Another point of interest is the angle ϕ_y , at which the maximum radiation intensity occurs for a non-optimal detune Δv and kick α . In order to arrive at a compact expression, we approximate the sinc² function as a Gaussian centered at 0 with the appropriate width, $\text{sinc}^2(x) \approx e^{-x^2/3}$. With this simplification the angle ϕ_y^* of maximum emission is the only real solution to

$$6N\phi_y^* = (\alpha - \phi_y^*)\pi N_u \left(\gamma_z^2 (\alpha - \phi_y^*)^2 + \Delta v \right), \quad (9)$$

where $N = k\sigma^2/L_u$ is the electron beam Fresnel number [4]. This simplification ignores the local maxima of the sinc function that occur away from the origin, though similar equalities could be written for these maxima. Equation 9 is compared to Genesis simulation results with LCLS-like parameters in a subsequent section.

For beams with a large transverse size, $N \rightarrow \infty$, and therefore $\phi_y^* \rightarrow 0$. Such a beam will only radiate perpendicular to its microbunches.

For beams of small transverse size, $N \rightarrow 0$, and therefore $\phi_y^* \rightarrow \alpha + (\alpha\Delta v/|\alpha\Delta v|)|\Delta v|^{1/2}/\gamma_z$. In this regime, radiation at or beyond the kick angle α is possible.

The number of wiggle periods N_u is important in the intermediate regime where N is close to unity. N_u governs how sharp the sinc² function is. Thus, a long undulator will have more concentrated off-axis emission.

A MECHANISM TO TILT MICROBUNCHES

The previous section showed that off-axis emission from a tilted microbunch is predicted from classical radiation theory. In this section, however, we show that a microbunch kicked off-axis is expected to realign towards the new direction of travel. This effect is not large, but may be large enough to extend the off-axis radiation farther off axis. This realignment is the result of an interaction with an extant electric field.

For simplicity we consider the dynamics of an electron moving in a diffracting Gaussian field E are described by the FEL pendulum equations [2],

$$\frac{d\theta}{dz} = 2k_u\eta \quad (10)$$

$$\frac{d\eta}{dz} = 2\chi_1 E(y, z) \quad (11)$$

$$E(y, z) = \frac{E_0 w_0}{w(z)} e^{-y(z)^2/w(z)^2} \cos(\psi(z) + \theta), \quad (12)$$

where θ is the electron phase, $\eta = (\gamma - \gamma_0)/\gamma_0$ is the energy deviation, $\chi_1 = Ke/\sqrt{2}\gamma_0 mc^2$, w_0 is the beam waist size, $w(z)^2 = w_0^2(1 + z^2/z_r^2)$, $z_r = \pi w_0^2/\lambda$ is the Rayleigh range, and

$$\psi(z) = \tan^{-1}\left(\frac{z}{z_r}\right) - \frac{ky(z)^2}{2z(1 + z_r^2/z^2)}. \quad (13)$$

The FEL resonance condition eliminates the $kz - \omega t$ phase accrual in an electric field, but the Gouy phase $\tan^{-1}(z/z_r)$ and the off-axis term in $\psi(z)$ cannot be accounted for by a wiggler with a constant K value. Equation 12 is written with $z = 0$ corresponding to the Gaussian beam waist. While the actual beam waist is behind the end of an undulator, we argue momentarily that the curvature of the field not critical under LCLS-like conditions, and the exponential drop-off in intensity plays a more important role. The FEL pendulum equations are usually written with a third differential equation relating the field growth to the bunching. In this analysis we ignore this effect, and therefore the result is not self-consistent. We believe the model still provides some understanding of the phenomena observed in simulation, so we proceed. In analogy to Figure 1, only the radiation from undulators upstream of the kick will affect the particle dynamics discussed here.

We will also assume that the transverse position of the electron is simply

$$y(z) = \alpha z + y_0. \quad (14)$$

This trajectory ignores undulator focusing and transverse field effects. Equations 10-12 can easily be solved numerically, but insight is gained from making two assumptions.

The first simplification is that the electron is kicked far beyond a beam waist after propagating a distance z_r ,

$$\alpha \gg \frac{w_0}{z_r} = \frac{\lambda}{\pi w_0}. \quad (15)$$

During Delta experiments, this criterion is weakly satisfied. Typical values for α are around 30–60 μrad , while matching simulations at 850 eV tells us that $\lambda/(\pi w_0) \approx 15 \mu\text{rad}$.

The assumption in Equation 15 means the exponential factor in Equation 12 will have turned off any interaction long before an electron travels a Rayleigh range. Therefore, the phase factor

$$\psi(z) = \tan^{-1}\left(\frac{z}{z_r}\right) - \frac{k(y_0 + \alpha z)^2}{2z(1 + z_r^2/z^2)} \quad (16)$$

is zero for the duration of interaction when $y_0 = 0$.

A corollary is $y_0 \ll \alpha z_r$, generalizing the previous statement to include non-zero y_0 . This follows directly from Equation 15 since a typical electron transverse starting position is of the same order as w_0 .

The second assumption is that the phase θ in Equation 12 may be treated as constant. This may be justified by requiring that the phase, θ_e , accumulated over the distance

at which $E(y, z)$ is decreased by $1/e$ is small. It follows from Equations 10-12 that, for $y_0 = 0$,

$$|\theta_e| < 2\chi_1 |E_0| k_u \frac{w_0^2}{\alpha^2} \left(\frac{1}{e} - 1 + \sqrt{\pi} \text{Erf}(1) \right), \quad (17)$$

where $\text{Erf}(x)$ is the error function. Since $|y_0| \lesssim w_0$, this argument still holds for nonzero y_0 . For the LCLS-like situation analyzed in the subsequent section, the left hand side of the inequality evaluates to 0.26.

With these two assumptions, Equations 10 and 11 take a much simpler form,

$$\frac{d\theta}{dz} = 2k_u \eta \quad (18)$$

$$\frac{d\eta}{dz} = 2\chi_1 E_0 e^{-(y_0+\alpha z)/w_0^2} \cos \theta_0. \quad (19)$$

These equations have simple solutions expressed in terms of the error function. Of interest here is the microbunch angle, $\alpha_b = -(k)^{-1} d\theta/dy$ at a particular location z . The on-axis ($y_0 = 0$) angle is

$$\alpha_{b,y_0=0} = \frac{E_0 \chi_1 w_0}{\alpha^2 \gamma_z^2} \left(2 \frac{z\alpha}{w_0} - \sqrt{\pi} \text{Erf} \left(\frac{z\alpha}{w_0} \right) \right) \cos \theta_0. \quad (20)$$

The scaling with z is somewhat hidden by the error function, but the rate at which the slope changes with z is more elucidating,

$$\left. \frac{d\alpha_b}{dz} \right|_{y_0=0} = \frac{2E_0 \chi_1}{\alpha \gamma_z^2} \left(1 - e^{-z^2 \alpha^2 / w_0^2} \right) \cos \theta_0. \quad (21)$$

Evidently after a quick energy modulation for $z \lesssim w_0/\alpha$, the microbunches continue to shear. The shearing continues indefinitely in this model, similar to the first step in the EEHG scheme [6]. However, a non-zero energy spread and emittance, not included here, will also rapidly debunch the beam.

Another feature of note is the importance of the initial phase, θ_0 . When operating the Delta undulator, a phase shifter immediately before the wiggler allows for a particular phase, and therefore tilt.

A quantitative comparison of Equation 20 with Genesis simulations are shown in the next section.

COMPARISON WITH SIMULATION

In this section we compare the predictions of the previous sections with Genesis [7] simulations. The simulation conditions, seen in Table 1, were chosen to match experiments done at LCLS. In order to generate a useful test, a pre-microbunched beam is sent through a 3.2-m helical afterburner.

The beam is pre-microbunched in a reverse tapered LCLS-like undulator 9 undulator segments in length. This reverse tapered undulator generates a microbunched beam and 0.34 GW of background, linearly polarized radiation. This background field is decomposed into right and left circular components, and sent into a helical afterburner with variable K .

Table 1: Simulation Parameters

Parameter	Value
Beam energy	4.37 GeV
Energy spread	1.8 MeV
Photon energy	850 eV
Peak current	2.5 kA
Emittance	0.4 μm
Afterburner length	3.2 m

The predicted detune required for maximum power, Equation 8, is compared with the radiation produced in the helical afterburner in Figure 2. The coherent radiation model matches simulation even though the afterburner is more than a gain length long. The prediction (dashed) is compared with Genesis results (solid) for $\alpha = 30 \mu\text{rad}$ and $\alpha = 60 \mu\text{rad}$. A 0- μrad K -scan is shown for comparison.

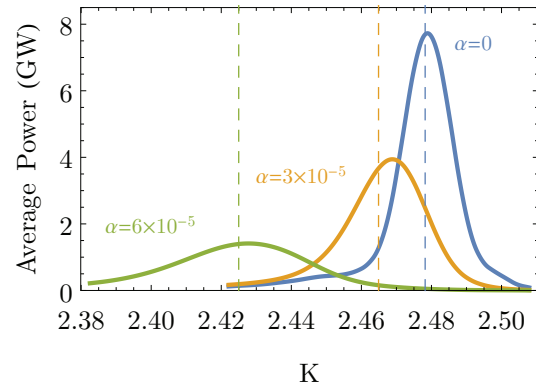


Figure 2: The average power from a Genesis simulation output as a function of afterburner K . A kick of $60 \mu\text{rad}$ (green), $30 \mu\text{rad}$ (orange), and $0 \mu\text{rad}$ (blue) are plotted along with the prediction from Equation 8.

Figure 3 compares the predicted angle at which the power is maximized, Equation 9, with the simulated angle at which power is maximized for $\alpha = 30 \mu\text{rad}$. The prediction fails at a large positive detune because the sinc^2 function's secondary local maxima are ignored in Equation 9.

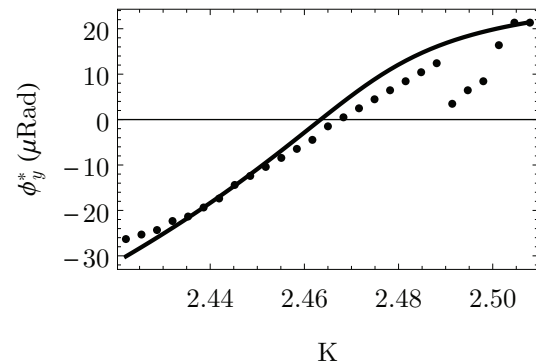


Figure 3: The angle of maximum emission as a function of K value is plotted for $\alpha = 30 \mu\text{rad}$. Genesis results are dots, while the solid line is Equation 9.

Content from this work may be used under the terms of the CC BY 3.0 licence (© 2018). Any distribution of this work must maintain attribution to the author(s), title of the work, publisher, and DOI.

Figure 4 compares the predicted microbunch angle, Equation 20, with the microbunch angle observed in Genesis simulations after a 30- μ rad kick. The phase is set to $\theta_0 = 0$ for comparison. The microbunch angle is calculated from the Genesis output file by performing an angular transform on the complex bunching factor for each output slice, and averaging over all slices. In this way the average angle is automatically weighted by the strength of the bunching in a given slice.

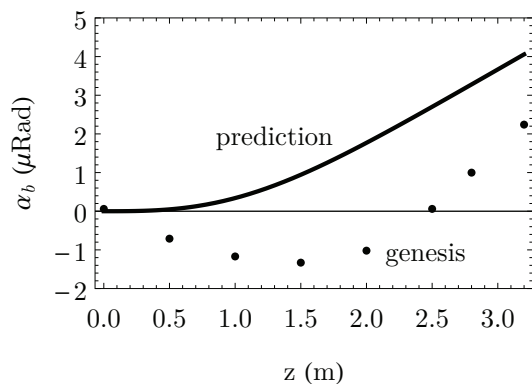


Figure 4: The predicted microbunch angle (solid) is plotted against the microbunch angle calculated from a Genesis output (dots).

REFERENCES

- [1] A. A. Lutman *et al.*, “Polarization control in an X-ray free-electron laser,” *Nat. Photon.*, vol. 10, p. 468, May 2016.
- [2] K. Kim, Z. Huang, and R. Lindberg, *Synchrotron Radiation and Free-Electron Lasers*. Cambridge, UK: Cambridge University Press, 2017.
- [3] T. Tanaka, H. Kitamura, and T. Shintake, “Consideration on the BPM alignment tolerance in X-ray FELs,” *Nucl. Instr. Meth. Phys. Res.*, vol. 528, p. 172, Aug. 2004.
- [4] E. L. Saldin, E. A. Schneidmiller, and M. V. Yurkov, “A simple method for the determination of the structure of ultrashort relativistic electron bunches,” *Nucl. Instr. Meth. Phys. Res.*, vol. 539, p. 449, Mar. 2005.
- [5] G. Geloni, V. Kocharyn, and E. Saldin, “On radiation emission from a microbunched beam with wavefront tilt and its experimental observation,” arXiv 1706.10185, Jun. 2017.
- [6] G. Stupakov, “Using the beam-echo effect for generation of short-wavelength radiation,” *Phys. Rev. Lett.*, vol. 539, p. 449, Mar. 2005.
- [7] S. Reiche, “GENESIS 1.3: a fully 3D time-dependent FEL simulation code,” *Nucl. Instr. Meth. Phys. Res.*, vol. 102, p. 074801, Feb. 2009.